Chiang Mai J. Sci. 2019; 46(3) : 618-625
http://epg.science.cmu.ac.th/ejournal/
Contributed Paper

Optical Absorption and FTIR Study of Cellulose/TiO_2 Hybrid Composites

Kittiya Plermjai [a], Kanokthip Boonyarattanakalin [a], Wanichaya Mekprasart [a], Weerachon Phoohinkong [b], Sorapong Pavasupree [c] and Wisanu Pecharapa* [a]

[a] College of Nanotechnology, King Mongkut's Institute of Technology Ladkrabang, Bangkok 10520, Thailand.

[b] Faculty of Science and Technology, Suan Dusit University, Bangkok, 10700, Thailand.

[c] Department of Materials and Metallurgical Engineering, Faculty of Engineering, Rajamangala University of Technology Thanyaburi, Klong 6, Pathumthani 12110, Thailand.

*Author for correspondence; e-mail: kpewisan@gmail.com, Wisanu.pe@kmitl.ac.th

Received: 22 February 2019
Revised Date: 18 April 2019
Accepted: 22 April 2019

Abstract

Cellulose/TiO_2 composite was prepared by conventional mixing using distilled water as medium. The structure and relevant properties of cellulose/TiO_2 composite were characterized by X-ray diffraction (XRD), Fourier Transform Infrared Spectroscopy (FTIR) and UV- Vis spectroscopy. XRD results exhibit typical cellulose structure type I. The absorbance spectra of TiO_2 and cellulose exist in vicinity of 200 nm and 350 nm in the UV range, corresponding to the UV-C, UV-B and UV-A. In addition, the UV absorption band of the composite can be extended covering wide UV region. Corresponding FTIR results suggest the existence of chemical bonding or surface interaction between TiO_2 and cellulose.

Keywords: titanium dioxide, cellulose, composite, FTIR

1. Introduction

Nowadays, organic-inorganic composite materials express new unique properties promising for superior performance in wide range of applications and emerging advanced technology. Cellulose /Titanium dioxide (TiO_2) composite as potential organic-inorganic material has gained considerable interest in several applications including self-cleaning materials, UV shielding materials, and air purification filters [1-3]. Natural cellulose is typically a polymer of β-(1→4)-D-glucopyranose with abundant surface hydroxyl groups forming plentiful inter- and intra- molecular hydrogen bonds. These hydroxyl groups provide suitable substrate for metal oxide incorporation onto the cellulose surface [4]. TiO_2 nanoparticles have attracted considerable attention because of the exceptional properties including wide optical band gap, strong ultraviolet absorptivity, non-toxicity, good chemical stability, excellent photocatalysis and high energy conversion efficiency [5]. TiO_2 naturally exists in three main phases: anatase, rutile, and brookite with different energy band gaps of about 3.2, 3.0 and 3.3 eV, respectively. These absorption energies are according to ultraviolet (UV) range to visible

edge at around 416 nm [6-7]. In this work, the TiO_2 (P25) powder containing mixed anatase and rutile phases was used as an inorganic component to prepare an organic-inorganic material composite.

Furthermore, an incorporation of small amount of functional organic-inorganic composite can significantly improve mechanical, thermal and optical properties of host matrix [10]. The aim of the present work is proposed to study optical absorption and interaction between the cellulose and TiO_2 in form of organic-inorganic hybrid nanocomposite materials.

2. MATERIAL AND METHOD

2.1 Material

Sugarcane bagasse was collected from a factory located at Singburi province, Thailand and was used as a starting source of cellulose. Titanium dioxide (P25) was purchased from Sigma Aldrich.

2.2 Method

Cellulose was prepared from sugarcane bagasse by ball-milling-assisted acid hydrolysis process [11]. The cellulose/TiO_2 composite material was prepared from the extracted cellulose and TiO_2 nanoparticles. 0.5 % (w/v) of cellulose nanofibrils (CNF) was dispersed in distilled water at room temperature using mechanical stirring at 500 rpm for 1h. Then 0.5% (w/v) of TiO_2 nanoparticles were mixed and dispersed in the cellulose stock. The mixture was prepared at room temperature by stirring at 500 rpm for 1h. The final suspension was casted onto PET substrate and dried at 40 °C for 12 h to remove water and moisture before characterization.

2.3 Characterizations

The chemical constituents of cellulose, TiO_2 and the composite were investigated by Fourier Transform Infrared (FTIR) spectroscopy (Thermo Scientific Nicolet 6700). The FTIR spectra were recorded in the region between 4000 and 400 cm^{-1}. The crystalline structure and phase identification of the cellulose composites were investigated by X-ray diffraction (Rigaku, Smart lab). The optical transmittance of the prepared films was measured from 190 to 700 nm using UV-Vis spectrometer (PG, T90+).

3. RESULTS & DISCUSSIONS

3.1 Crystallinity Analysis

Figure 1 shows the XRD patterns of cellulose, TiO_2 and cellulose/TiO_2 composite. In Figure 1 (a), peaks at 16.2° and 22.2° correspond

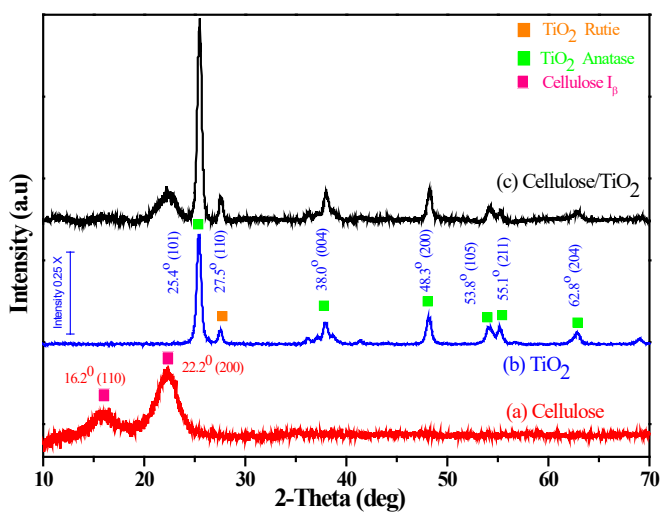

Figure 1 XRD pattern of (a) cellulose, (b) TiO_2 and (c) cellulose/TiO_2.

to the (110) and (200) lattice planes, respectively. These peaks are attributed to typical crystal lattice of cellulose I_β. XRD spectra of the P25 (Figure 1(b)) confirm the presence of anatase along with rutile phase. Several characteristic peaks attributing to anatase at 25.4°, 38.0°, 48.3°, 53.8° and 62.8° are observed. The small peak at 27.5° corresponds to the typical rutile phase. This XRD pattern is in good agreement with the standard diffraction data (JCDS 21-1272 and 21-1276). The calculated weight fraction between anatase and rutile from the integrated intensity peaks of anatase (101) and rutile (110) were 90.7% and 9.3 %, respectively [12]. The cellulose/TiO_2 composite (Figure 1(c)) shows the high intensity XRD pattern of TiO_2, which indicates the high crystalline anatase phase according to the starting TiO_2 phase fraction [13]. No any significant changes in the XRD patterns of both TiO_2 and cellulose in the composite.

3.2 FTIR Spectroscopic Analysis

Cellulose I_β is long chain polysaccharide, composed of β-1,4-linked D-glucopyranoside units as shown in Figure 2(a). Linear β-D-glucopyranoside chains are connect to parallel adjacent chains by hydrogen bonds (O-H···O) as shown in Figure 2(b). Hydrogen bonds involving OH at the C-2, C-3, and C-6 positions play key roles in the packing of cellulose chain to a particle of cellulose crystal. Each sheet of β-D-glucopyranoside chain are stacked and connected to neighboring layer by van der Waals hydrophobic interaction between pyranose ring without any hydrogen bonds along an a-axis. The formation of hydrogen bonds reflects cellulose information of amorphous, crystallinity, and crystallographic structure. Moreover, the packing of microfibril via surface hydroxyl groups and the interactions between cellulose surface hydroxyl groups and metal oxide surface can be also examined by the hydrogen bond formations [14-18]. In this study the FTIR spectra were deconvoluted by using curve fitting method in order to carefully investigate in the region of OH stretching modes.

The overall IR spectra of cellulose (a), cellulose/TiO_2 (b) and TiO_2 (c) in the range between 4000-400 cm^{-1} are shown in Figure 3. The board band at 3600–3000 cm^{-1} refers to the stretching vibration of hydroxyl groups of cellulose chain via both inter- and intra-molecular hydrogen bonds [14-16] contributing with hydroxyl groups of water molecules. The presence of O-H bending vibration mode of the peak position at around 1600 cm^{-1} confirms the existence of adsorbed water molecules

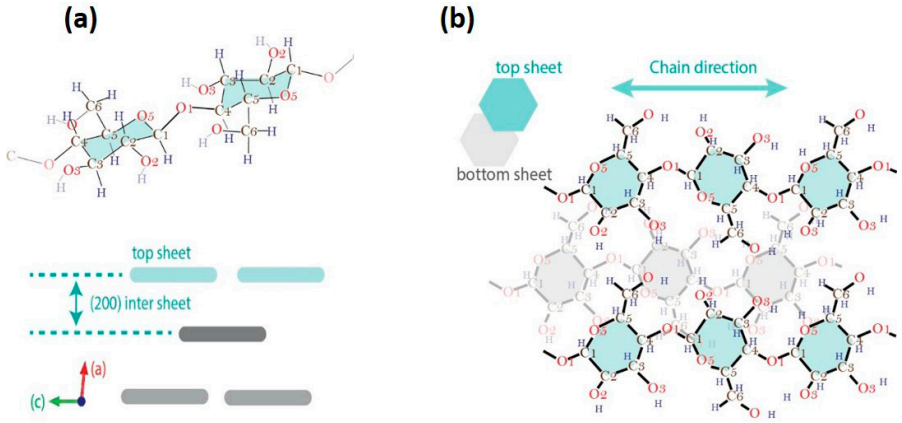

Figure 2 (a) Cellulose I_β crystal structure model [32] with (200) plane due to intersheet spacing projection on b-direction and (b) part of cellulose chain molecule in cellulose sheet projection on a-direction.

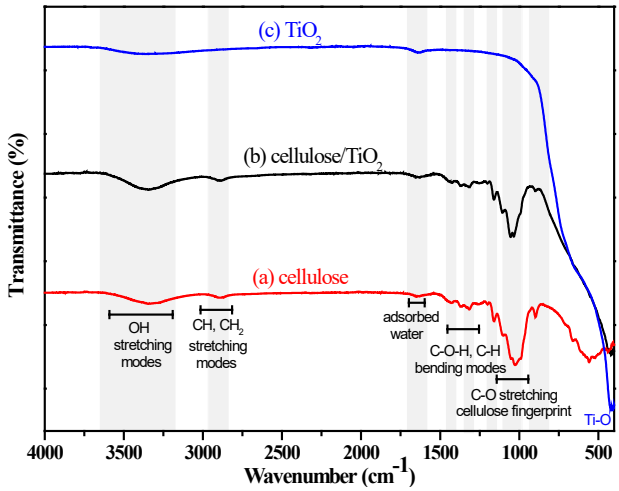

Figure 3 FTIR spectra of (a) cellulose, (b) cellulose/TiO_2 and (c) TiO_2.

in all samples. The absorption band range at around 2830 cm^{-1} to 2970 cm^{-1} corresponds to the C-H, CH_2 stretching vibration of cellulose [17-21] which is not detected in the starting TiO_2 sample. The peaks between 1250 and 1450 cm^{-1} are assigned to the bending vibrational mode of CH_2 wagging and rocking with C-C-H and C-O-H bending modes [33, 34, 36]. The cellulose fingerprint absorption region around 930 to 1160 cm^{-1} is attributed to C-O-C and C-O stretching vibrational mode of cellulose structure [14, 16-18]. The strong peak intensity at around 400-800 cm^{-1} is characteristic of metal oxide Ti-O bond which is presented in both TiO_2 and cellulose/TiO_2 composite. The results confirm the existence of TiO_2 particle on cellulose composite sample.

Figure 4 presents the deconvoluted bands of OH stretching region of intra- and inter-molecular hydrogen bonds in crystalline, amorphous and surface hydroxyl groups of cellulose. The deconvoluted peak in this region can be used to confirm the characteristic of cellulose I_β. The curve fitting method deconvoluted the IR band in this region into seven bands [14-15, 18-23]. The main characteristic peak of cellulose I_β at 3253 cm^{-1} is assigned as an inter-chain hydrogen bond interaction of O6-H···O3 [14,15]. While the intra- molecular hydrogen bonds of O2-H···O6 and O3-H···O5 are found at 3288 and 3392 cm^{-1}, respectively [15,19, 30]. The deconvoluted peak at 3170 cm^{-1} is attributed by the stretching mode of O3-H hydroxyl group. The deconvoluted peak at 3341 cm^{-1} is contributed by O-H stretching in O6-H···O3-H···O5 hydrogen bond network. The broad peak at 3489 cm^{-1} due to the hydrogen bond formation of O2, O3, and O6 hydroxyl groups at an amorphous cellulose surface. The last deconvoluted peak at around 3590 cm^{-1} was contributed to water molecules and free surface OH group [14, 15, 23]. After incorporated with nanoTiO_2, the shift of cellulose OH stretching peaks corresponding to both inter- and intramolecular hydrogen bonds are observed. The change of inter- and intra-molecular hydrogen bond conformation may come from the interactions between surface O3 and O6 hydroxyl groups and TiO_2 surface. All possible inter- and intramolecular hydrogen bonds and possible interface between cellulose and TiO_2 surface are shown in Figure 5(a) and 5(b) [24-27]. In bare nanoTiO_2 sample, surface OH group signal is observed [24,25]. It is suggested that the hydrogen bond formation between surface TiO_2 and surface cellulose hydroxyl groups result in less flexibility of surface hydroxyl groups of cellulose. The strong intramolecular H-bonds

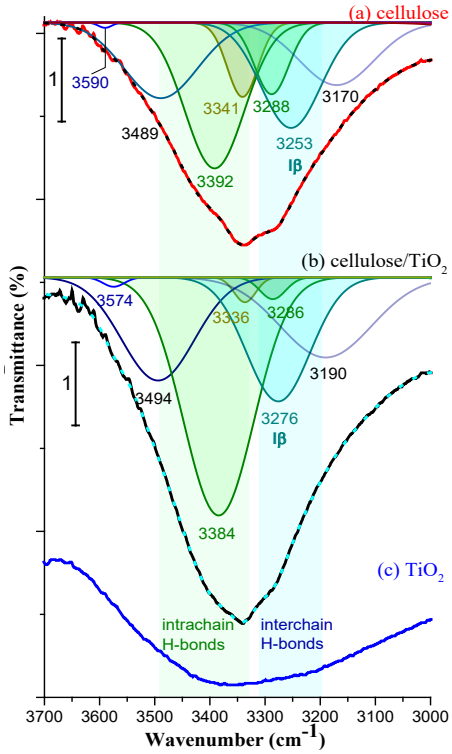

Figure 4 FTIR spectra of (a) cellulose, (b) cellulose/TiO_2, and (c) TiO_2 in the region of OH stretching vibration.

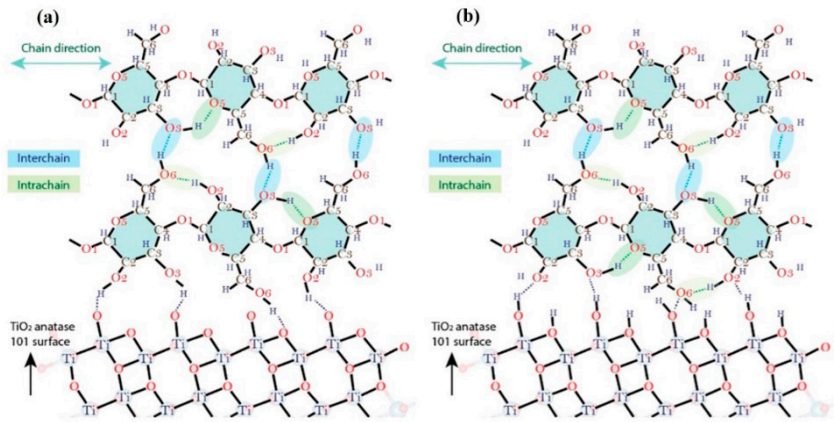

Figure 5 Two possible inter- and intra-molecular hydrogen bonds network between cellulose and TiO_2 surface.

at the interface is confirmed by the increasing of an intensity of the intrachain H-bond peak and the shift to higher energy region.

3.3 Optical Spectra Analysis

The wavelength range of optical radiation with shorter wavelength than 400 nm, namely UV radiation, consists of three bands which are 1) 100-280 nm (UVC), 2) 280-315 nm (UVB), and 3) 315-400 nm (UVA). The UV absorbance spectra of cellulose, TiO_2 and cellulose/TiO_2 were measured in the wavelength range of 190-700 nm and the corresponding results are shown in Figure 6. As observed in the UV

region ranging from 190-350 nm, cellulose, TiO_2 and cellulose/TiO_2 have strong absorbance peaks at around 190-220, 220-330 nm and 210-330 nm corresponding to UVC, UVB and UVA spectra, respectively. This result indicates that the enhanced feature in absorptivity of cellulose/TiO_2 hybrid composite could be correlated to strong absorbance character of both cellulose and TiO_2 which may be utilized as UV absorption materials for all UV-A, UV-B and UV-C range. Furthermore, the absorbance of cellulose/TiO_2 composite is significantly increased at the ultraviolet region corresponding to TiO_2 characteristics of both anatase and rutile phases. As noticed in figure 6(b), the UV-Vis transmittance spectra of cellulose/TiO_2 composite exhibit superiority in UV shielding efficiency accompanying the decrease in transmittance at around 15% in the wavelength vicinity of 200-330 nm.

The direct optical band gap energies of the cellulose, TiO_2 and cellulose/TiO_2 were

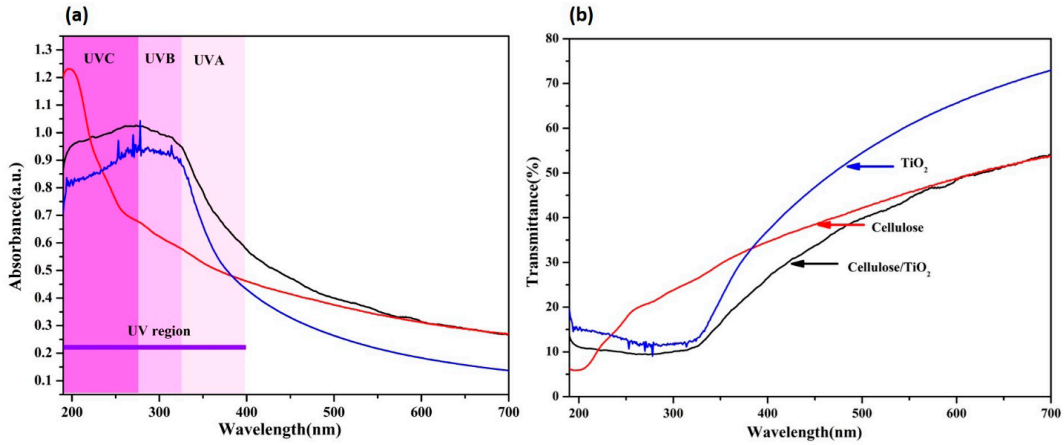

Figure 6. (a) UV-Vis absorbance spectra of cellulose, TiO_2 and cellulose/ TiO_2 (b) UV-Vis transmittance spectra of cellulose, TiO_2 and cellulose/ TiO_2

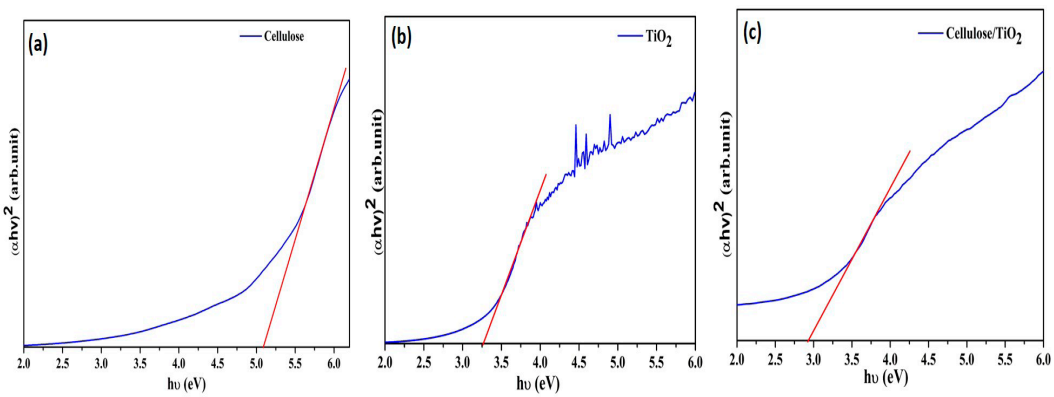

Figure 7. Optical properties of (a) cellulose, (b) TiO_2 and (c) cellulose/ TiO_2.

evaluated using the Tauc's relation as expressed in equation (1).

$$\alpha hv = A(hv - E_g)^{1/2}. \qquad (1)$$

Noted here that, hv is a photon energy, E_g is band gap energy, A is constant. The band gap energy was evaluated from the plot of $(ahv)^2$ and as shown in Figure 7 (a) and (b) respectively. The calculated optical band gap of cellulose,

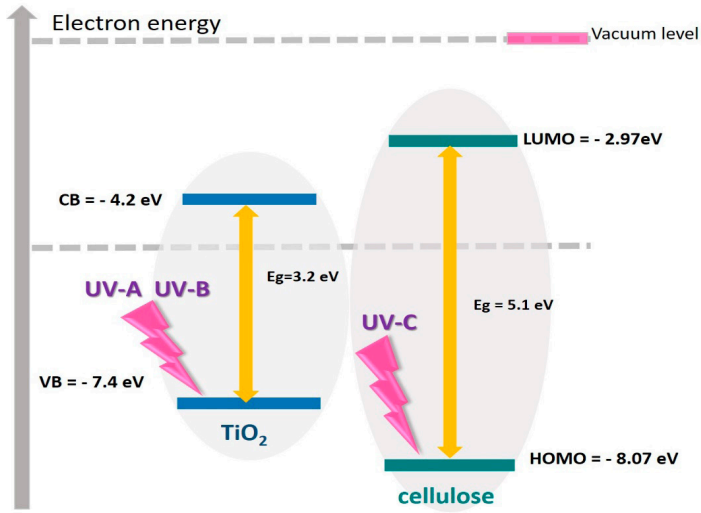

Figure 8 The energy band diagram of cellulose and TiO_2.

TiO_2 and cellulose/TiO_2 were found to be 5.1 eV, 3.2 eV and 2.93 eV, respectively. The corresponding electronic level and vacuum level energy are illustrated in Figure 8. Typically, the energy levels of conduction band and valence band of TiO_2 are located at -4.2 and -7.4 eV below vacuum level, respectively [28] meanwhile the highest occupied molecular orbital (HOMO) level of cellulose is approximately -8.07 eV [29] with respect to vacuum level that is lower than the valence band of TiO_2 and LUMO level is situated at -2.97 eV below vacuum level which is higher than the conduction band of TiO_2. As a result, it is suggested that the integration of cellulose and TiO_2 can improve UV-shielding efficiency because of the increase in ultraviolet absorptivity of both materials.

4. Conclusions

In summary, cellulose/TiO_2 hybrid composite was prepared by mixing method and it exhibited strong absorbance in UV-A, UV-B and UV-C region. FTIR results suggest that cellulose may interact with TiO_2 by inter- and intramolecular hydrogen bonds existing at their interface. The lower band gap energy of cellulose/TiO_2 hybrid composite, comparing with bare TiO_2 and cellulose, at around 2.93 eV is strongly correlated to the change in the environment of cellulose surface hydroxyl groups by interactions with TiO_2 particle. It is suggested that the cellulose/TiO_2 composite may be utilized as a UV blocking material due to enhancement in its UV absorption performance comparing to bare cellulose and TiO_2.

Acknowledgments

This work has partially been supported by the National council of Thailand (Grant No 488072) for financial support and College of nanotechnology King Mongkut's Institute of Technology Ladkrabang.

Reference

[1] Marques P.A.A.P., Trindade T. and Neto C.P., *Compos. Sci. Technol.*, 2006; **66**: 1038-1044. DOI 10.1016/j.compscitech.2005.07.029

[2] Oliveira A. C.M., Santos M.S., Brandão L.M.S., Resende I.T.F., Leo I.M., Morillo E.S., Yerga R.M.N., Fierro J.L.G., Egues S.M.S. and Figueiredo R.T., *Int. J. Hydrogen Energ.*, 2017; **4**: 28747-28754. DOI.org/10.1016/j.ijhydene.2017.09.022

[3] Keshk S.M.A.S., Hamdy M.S. and Badr I.H.A., *Am. J. Polym. Sci.*, 2015; **5(1)**: 24-29. DOI: 10.5923/j.ajps.20150501.04

[4] Santos D.A., Oliveira M.M., Curvelo A.A.S., Fonseca L.P. and Porto A.L.M., *Int. Biodeter. Biodegr.*, 2017; **121**: 66-78. DOI.org/10.1016/j.ibiod.2017.03.014

[5] Simpraditpan A., Wirunmongkol T., Boonwatcharapunsakun W., Pivsa-Art S., Duangduen C., Sakulkhaemaruethai S. and Pavasupree S., *Enrgy Procedia*, 2011; **9**: 440-445. DOI: 10.1016/j.egypro.2011.09.049

[6] Ge M., Cao C., Huang J., Li S., Chen Z., Zhang K.Q., Al-Deyab S.S. and Lai Y., *J. Mater. Chem. A*, 2016; **4**: 6772-6801. DOI: 10.1039/C5TA09323F

[7] Zhang Y., Jiang Z., Huang J., Lim L.Y., Li W., Deng J., Gong D., Tang Y., Lai Y. and Chen Z., *RSC Adv.*, 2015; **5(97)**: 79479-79510. DOI: 10.1039/c5ra11298b

[8] Ohno T., Sarukawa K., Tokieda K. and Matsumura M., *J. Catal.*, 2001; **203**: 82-86. DOI:10.1006/jcat.2001.3316

[9] Nussbaumer R.J., Caseri W.R., Smith P. and Tervoort T., *Macromol. Mater. Eng.*, 2003; **288**: 44-49. DOI: 10.1002/mame.200290032

[10] Pavlidou S. and Papaspyrides C.D., *Prog. Polym. Sci.*, 2008; **33**: 1119-1198. DOI:10.1016/j.progpolymsci.2008.07.008

[11] Plermjai K., Boonyarattanakalin K., Mekprasart W., Pavasupree S., Phoohinkong, W. and Pecharapa W., *AIP Conf. Proc.*, 2018; **2010**: 020005-1 - 020005-7 DOI: 10.1063/1.505318

[12] Ananpattarachai J., Kajitvichyanukul P. and Seraphin S., *J. Hazard. Mater.*, 2009; **168**: 253-261. DOI:10.1016/j.jhazmat.2009.02.036

[13] Moon R.J., Martini A., Nairn J., Simonsen J. and Youngblood J., *Chem. Soc. Rev.*, 2011; **40**: 3941-3994. DOI: 10.1039/c0cs00108b

[14] Ivanova N.V., Korolenko E.A., Korolik E.V. and Zhbankov R.G., *J. Appl. Spectrosc.*, 1989; **51**: 847-851. DOI: 10.1007/BF00659967

[15] Kondo T., *Cellulose*, 1997; **4**: 281-292. doi.org/10.1023/A:1018448109214

[16] Barsberg S., *J. Phys. Chem. B*, 2010; **114**: 11703-11708. DOI: 10.1021/jp104213z

[17] Agarwal V., Huber G.W., Conner Jr W.C. and Auerbach S.M., *J. Chem. Phys.*, 2011; **135**: 134506 (12pp). DOI: 10.1063/1.3646306

[18] Kim S.H., Lee C.M. and Kafle K., *Korean J. Chem. Eng.*, 2013; **30**: 2127-2141. DOI: 10.1007/s11814-013-0162-0

[19] Lee C.M., Mohamed N.M.A., Watts H.D., Kubicki J.D. and Kim S.H., *J. Phys. Chem. B.*, 2013; **117**: 6681-6692. DOI.org/10.1021/jp402998s

[20] Chen C., Luo J., Qin W. and Tong Z., *Monatsh. Chem.*, 2014; **145**: 175-185. DOI 10.1007/s00706-013-1077-5

[21] Lee C.M., Kafle K., Park Y.B. and Kim S.H., *Phys. Chem. Chem. Phys.*, 2014; **16(22)**: 10844-10853.

[22] Kubicki J.D., Watts H.D., Zhao Z. and Zhong L., *Cellulose*, 2014; **21**: 909-926. DOI 10.1007/s10570-013-0029-x

[23] Lee C.M., Kubicki J.D., Fan B., Zhong L., Jarvis M.C. and Kim S.H., *J. Phys. Chem. B.*, 2015; **119(49)**: 15138-15149.

[24] Ahmadizadegan H., *J. Colloid. Interf. Sci.*, 2017; **491**: 390-400.

[25] Martakov I.S., Torlopov M.A., Mikhaylov V.I., Krivoshapkina E.F., Silant'ev V.E. and Krivoshapkin P.V., *J. Sol-Gel Sci. Technol.*, 2018; **88**: 13-21.

[26] Islam M.S., Chen L., Sisler J. and Tam K.C., *J. Mater. Chem. B*, 2018; **6**: 864-883.

[27] Mohamed M.A., Abd Mutalib M., Mohd Hir Z.A., M. Zain M.F., Mohamad A.B., Jeffery M.L., Awang N.A. and Salleh W.N., *Int. J. Biol. Macromol.*, 2017; **103**: 1232-1256.

[28] Mekprasart W., Vittayakorn N. and Pecharapa W., *Mater. Res. Bull.*, 2012; **47**: 3114-3119.

[29] Simão C.D., Reparaz J.S., Wagner M.R., Graczykowski B., Kreuzer M., Ruiz-Blanco Y.B., García Y., Malho J.M., Goñi A.R., Ahopelto J. and Sotomayor T.C.M., *Carbohydr. Polym.*, 2015; **126**: 40-46.